Efficient nonclassical state preparation via generalized parity measurement

Chen-yi Zhang¹ and Jun Jing^{1,*}
¹School of Physics, Zhejiang University, Hangzhou 310027, Zhejiang, China
(Dated: August 21, 2025)

Nonclassical states of bosonic modes, especially the large number states, are valuable resources for quantum information processing and quantum metrology. However, it is intricate to apply unitary protocols to generate a desired Fock state due to the uniform energy spectrum of bosonic system. We here propose a measurement-based protocol that leverages the resonant Javnes-Cummings interaction of the bosonic mode with an ancillary two-level atom and sequential projective measurements on the atom. Using the generalized parity measurement constructed by several rounds of free-evolution and measurement with proper intervals, we can efficiently filter out the unwanted population and push the target mode conditionally toward the desired Fock state. In ideal situation, a Fock state $|n_t \approx 2000\rangle$ can be prepared with a fidelity over 98% using only 8 rounds of measurements. With qubit dissipation and dephasing and cavity decay in the current circuit QED platforms, a Fock state $|n_t \approx 100\rangle$ can be prepared with a fidelity about 80% by 6 measurements. It is found that the number of the measurement rounds for preparing a large Fock state $|n_t\rangle$ scales roughly as $\log_2 \sqrt{n_t}$, similar to the number of ancillary qubits required in the state preparation via the quantum phase estimation algorithm yet costs much less gate operations. Our protocol can also be used to prepare a large Dicke state |J| < 1000, 0 of a spin ensemble with a sufficiently high fidelity by less than 3 measurements, which is qualified for the quantum Fisher information approaching the Heisenberg scaling in sensing the rotation phase along the x axis.

I. INTRODUCTION

Quantum measurement has a long history serving as a fundamental tool for controlling and manipulating quantum states. First rigorously analyzed by Misra and Sudarshan in 1977 [1], the sufficiently frequent projective measurements on an initial state can "frozen" the system in that state, which is known as the quantum Zeno effect (QZE) [2–4]. Closely associated with QZE, a purification protocol was proposed by performing a series of frequent measurements on a system to manipulate the dynamics of another system that is coupled to it [5, 6]. Following these pioneer works, numerous efforts have been devoted to exploiting Zeno-like measurements for various quantum control tasks, such as entanglement generation [7–10], ground state preparation [11–15], nuclear spin polarization [16, 17], and quantum battery charging [18].

More than merely exploiting the frequently measurements on the ancillary system, one can accelerate the state preparation by incorporating appropriate gate operations on the ancillary system into the joint free evolution. A widely adopted protocol leverages the quantum phase estimation (QPE) algorithm to prepare eigenstates of a unitary operator $U|u\rangle = e^{i2\pi\varphi}|u\rangle$ with eigenvalue $e^{i2\pi\varphi}$ and eigenstate $|u\rangle$ [19, 20]. In QPE, the target system of several qubits is coupled to a register of N ancillary qubits. By performing 2^N controlled unitary operators, the eigen-phase φ of the unitary operator is encoded into the ancillary register [21]. Then after an inverse quantum Fourier transform and the subsequent measurements on the ancillary qubits, the target system

is collapsed by the protocol to an eigenstate $|u\rangle$ of the unitary operator with a probability determined by its initial overlap with $|u\rangle$. The estimated eigen-phase can be written as a binary decimal:

$$\varphi = 0.\varphi_1 \varphi_2 \dots = \sum_{l=1}^{N} \varphi_l 2^{-l}, \tag{1}$$

where φ_l is the measurement outcome of the *l*th qubit, either zero or one.

Alternatively, one can implement the phase estimation using a single ancillary qubit by iterating a Ramsey-type circuit [22]. At the beginning of the kth round of protocols [23, 24] with $1 \le k \le N$, the ancillary qubit is reset as $(|0\rangle + |1\rangle)/\sqrt{2}$ via a Hadamard gate. Then 2^{k-1} controlled-U operations are applied to the target system. followed by a conditional single-qubit rotation along the z axis $R_z(a_k) = |0\rangle\langle 0| + e^{i2\pi a_k} |1\rangle\langle 1|$ of the ancillary qubit, where a_k is determined by the outcomes of all preceding measurements. After another Hadamard gate, the state of the ancillary qubit can be read out by a projective measurement. The system under such N rounds can be pushed to the vicinity of a desired or random eigenstate of the estimation unitary operator U (or a superposition of them) with an uncertainty of the estimated eigen-phase $\delta\varphi \propto 2^{-N}$. This uncertainty scaling is consistent with Eq. (1) in standard QPE [25]. This protocol has been used to prepare the Gottesman-Kitaev-Preskill state as an eigenstate of the displacement operator of the bosonic modes [25, 26], the Dicke state of a spin ensemble as an eigenstate of $U = \exp(-iJ_z)$ [27], and the large Fock state of the microwave cavity mode that is dispersively coupled to an ancillary transmon qubit [28].

In this work, we propose a protocol for generating nonclassical quantum states in the Hilbert space of high

^{*} Contact author: jingjun@zju.edu.cn

dimensionality via effectively constructing a generalized parity measurement (GPM) by optimizing the time intervals between Zeno-like measurements. The required number of measurement rounds exhibits a logarithmic scaling similar to the number of ancillary qubits in quantum phase estimation algorithms: $N \sim \log_2 n_t$, where n_t indicates the target number state or the excitation number uncertainty $\sqrt{n_t} = |\alpha|$ when the target resonator (bosonic mode) is initially prepared as a coherent state $|\alpha\rangle$. Our protocol exploits the resonant exchange coupling between the target resonator and the ancillary twolevel system (TLS) and the projective measurements on TLS, which is more convenient than the protocols based on QPE in gate operations and holds a much faster speed of state preparation than the existing GPM protocol based on dispersive coupling [28, 29].

The rest of this paper is organized as follows. Sec. II A, we introduce the existing generalized parity measurement on the number state of the target bosonic mode based on the dispersive interaction between bosonic mode and ancillary TLS and the projective measurement on TLS. Then in Sec. IIB, we propose an efficient protocol to realize GPM through the resonant exchange interaction between bosonic mode and ancillary TLS and TLS measurement. In Sec. III, we present the results about the generation of a large Fock state in both ideal and realistic situations, which support an approximated logarithmic scaling of the measurement numbers as a function of the target number state. In Secs. IV A and IV B, we extend our protocol to generate the Dicke state of a spin ensemble with a similar GPM operator and demonstrate the protocol performance in both state preparation and its application in quantum metrology, respectively. The conclusion is provided in Sec. V.

II. THEORETICAL MODEL

A. Generalized parity measurement

To efficiently generate a large Fock state $|n_t\rangle$ with $n_t \gg 1$, a generalized parity measurement on the target resonator has been realized by the quantum circuit model in Fig. 1(a), which is a standard Ramsey-type sequence [22, 28]. In a modern cavity QED platform [28], the ancillary TLS (superconducting qubit) is dispersively coupled to the target resonator (a 3D microwave cavity single-mode) with a Hamiltonian ($\hbar = 1$)

$$H_{\rm dis} = \Delta |e\rangle \langle e| - \chi a^{\dagger} a |e\rangle \langle e|, \tag{2}$$

where $\Delta = \omega_q - \omega_a$ is the detuning between qubit and resonator, χ is the dispersive coupling strength, $|e\rangle$ is the excited state of the qubit, and a is the annihilation operator of the bosonic mode. Suppose that the initial state of the resonator is $|\psi_a\rangle = \sum_n C_n |n\rangle$. The qubit is initialized as $(|g\rangle + |e\rangle)/\sqrt{2}$ by a Hadamard gate. After a period of joint evolution governed by $e^{-iH_{\rm dis}\tau}$ with a

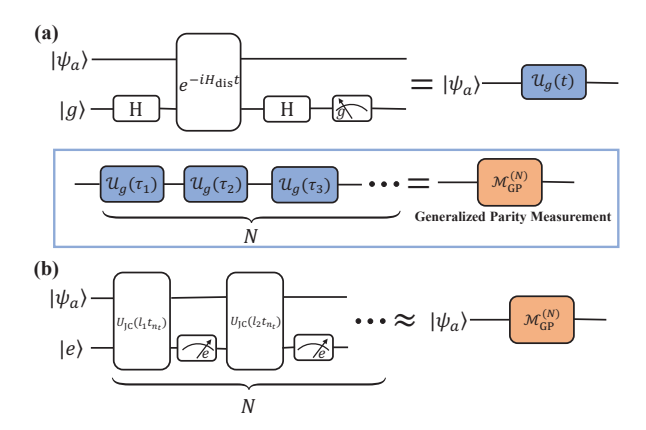


FIG. 1. (a) Circuit diagram for realizing GPM through free joint evolution of dispersively coupled resonator and ancillary TLS, the Hadamard gates on TLS, and the projective measurements on the ground state of TLS. (b) Circuit diagram of our protocol for constructing GPM on the target resonant by repeatedly measuring the excited state of the ancillary TLS, which is coupled to the resonator through exchange interaction

duration τ , the qubit obtains a relative phase relevant to the resonator states; and the state of the composite system becomes

$$\frac{1}{\sqrt{2}} \sum_{n=0}^{\infty} \left[|g\rangle + e^{-i(\Delta - \chi n)\tau} |e\rangle \right] C_n |n\rangle. \tag{3}$$

Then another Hadamard gate on the qubit gives rise to the state

$$\sum_{n=0}^{\infty} \frac{1}{2} \left[\left(1 + e^{-i(\Delta - \chi n)\tau} \right) |g\rangle + \left(1 - e^{-i(\Delta - \chi n)\tau} \right) |e\rangle \right] C_n |n\rangle.$$
(4)

Upon the projective measurement $M_g \equiv |g\rangle\langle g|$ on qubit, the quantum circuit [see the upper part of Fig. 1(a)] gives rise to a non-unitary evolution operator for the resonator

$$\mathcal{U}_g(\tau) = \sum_{n=0}^{\infty} e^{-i\frac{\Delta - \chi n}{2}\tau} \cos\left(\frac{\Delta - \chi n}{2}\tau\right) |n\rangle\langle n|, \quad (5)$$

when the measurement outcome turns out to be $|g\rangle$.

Then after N rounds of evolution, Hadamard gates, and measurement, the resonator state becomes

$$\rho_a(N) = \frac{\prod_{k=1}^N \mathcal{U}_g(\tau_k) \rho_a(0) \prod_{j=1}^N \mathcal{U}_g^{\dagger}(\tau_j)}{P(N)}, \qquad (6)$$

where $\rho_a(0)$ is an arbitrary initial density matrix, τ_k is the duration of the kth round, and P(N) is the success probability of obtaining the qubit in its ground state for multiple rounds. With $|n_t\rangle$ the target number state, one can set the detuning to be $\Delta = \chi n_t$ and the duration of the kth round as $\tau_k = \pi/(\chi 2^{k-1})$ [28, 29]. Then during

the kth round with $1 \leq k \leq N$, the population of the resonator outside the subspace of a general parity of 2^k , i.e., the set of Fock states $|n\rangle$ satisfying $|n-n_t|/2^k \in \mathbb{N}$, can be filtered out. On the whole, Eq. (6) is equivalent to performing a GPM on the resonator

$$\rho_a(N) = \frac{\mathcal{M}_{GP}^{(N)} \rho_a(0) \mathcal{M}_{GP}^{(N)}}{P(N)},\tag{7}$$

where the GPM operator is defined as

$$\mathcal{M}_{GP}^{(N)} \equiv \sum_{j \ge -|n_t/2^N|} |n_t + 2^N j\rangle \langle n_t + 2^N j|.$$
 (8)

If the resonator is prepared at a coherent state $\rho_a(0) = |\psi_a\rangle\langle\psi_a|$ with $|\psi_a\rangle = |\alpha\rangle = e^{-|\alpha|^2/2}\sum_{n=0}^{\infty}\alpha^n/\sqrt{n!}|n\rangle$, and it is assumed that $|\alpha|^2 = n_t$ to have the maximum initial overlap with the target state $|n_t\rangle$, then it is straightforwardly found that the number of protocol rounds required for generating the Fock state $|n_t\rangle$ scales roughly as $N_{\text{Fock}}(n_t) \sim \log_2 \sqrt{n_t}$, since the excitation number uncertainty is $\langle \Delta n \rangle = \sqrt{\langle n^2 \rangle - \langle n \rangle^2} = |\alpha| = \sqrt{n_t}$. This state-preparation protocol is similar to those based on QPE to project the system onto the eigenstate with zero eigen-phase of the unitary operator $U = e^{-i\pi(n_t - a^{\dagger}a)\chi}$.

B. Effective GPM in Jaynes-Cummings model under resonant condition

Inspired by the ideas of measurement-based cooling [11, 14] and charging [18], we find that an effective GPM operator similar to Eq. (8) can be constructed simply by sequentially performing projective measurements $M_e \equiv |e\rangle\langle e|$ to the ancillary TLS that is coupled to the target resonator via the Jaynes-Cummings interaction as shown in Fig. 1(b). In the rotating frame with respect to $\omega_a a^{\dagger} a$, the Hamiltonian reads

$$H_{\rm JC} = \Delta |e\rangle \langle e| + g\left(|e\rangle \langle g|a + |g\rangle \langle e|a^{\dagger}\right),\tag{9}$$

where g is the coupling strength. The ancillary two-level system is supposed to be prepared in the excited state $|e\rangle$. Then the initial state of the composite system is given by

$$\rho(0) = |e\rangle\langle e| \otimes \rho_a(0), \tag{10}$$

where $\rho_a(0)$ is the initial state of the resonator. After a period of joint evolution by $U_{\rm JC}(\tau)=\exp(-iH_{\rm JC}\tau)$ and if the measurement outcome is still $|e\rangle$, the resonator state turns out to be

$$\rho_a(1) = \frac{\Pi_e(\tau)\rho_a(0)\Pi_e^{\dagger}(\tau)}{P_e(1)},\tag{11}$$

where $P_e(1) = \text{Tr}[\Pi_e(\tau)\rho_a(0)\Pi_e^{\dagger}(\tau)]$ is the success probability of finding TLS at $|e\rangle$. $\Pi_e(\tau) \equiv \langle e|U_{\text{JC}}(\tau)|e\rangle$ is the

non-unitary evolution operator for the resonator, which reads

$$\Pi_e(\tau) = \sum_{n=0}^{\infty} \beta_n(\tau) |n\rangle \langle n|$$
 (12)

with coefficient

$$\beta_n(\tau) = e^{-i\Delta\tau/2} \left[\cos(\Omega_n \tau) + i \frac{\Delta}{2\Omega_n} \sin(\Omega_n \tau) \right], \quad (13)$$

where $\Omega_n \equiv \sqrt{\Delta^2/4 + (n+1)g^2}$ is the *n*-photon Rabi frequency. To attain a non-unitary evolution operator similar to Eq. (5) and to hold a target number state $|n_t\rangle$, we have $|\beta_{n_t}(\tau)| = 1$. This can be realized by setting the duration of the joint evolution to be

$$\tau = lt_{n_t}, \quad t_{n_t} \equiv \frac{\pi}{\Omega_{n_t}} \tag{14}$$

with $l \in \mathbb{N}$. By substituting Eqs. (14) and (13) into Eq. (12), the non-unitary evolution operator under resonant condition $\Delta = 0$ becomes

$$\Pi_e(\tau) = \sum_{n=0}^{\infty} \cos\left(l\pi\sqrt{\frac{n+1}{n_t+1}}\right) |n\rangle\langle n|.$$
 (15)

In this work, we restrict our attention to the generation of a large Fock state with $n_t \gg 1$ from a coherent state $|\alpha\rangle$ with $|\alpha|^2 = n_t$. Generally, the population of such a coherent state on the number state $|n\rangle$ can be negligible when $|n-n_t|\gg \sqrt{n_t}$. Consequently, in the regime of $|n-n_t| < \sqrt{n_t}$, we have

$$\Pi_{e}(\tau) = \sum_{n=0}^{\infty} \cos\left(l\pi\sqrt{\frac{n+1}{n_{t}+1}}\right)|n\rangle\langle n|$$

$$\approx \sum_{n=0}^{\infty} \cos\left[l\pi + l\pi\frac{n-n_{t}}{2(n_{t}+1)}\right]|n\rangle\langle n|$$

$$= (-1)^{l} \sum_{n=0}^{\infty} \cos\left[l\pi\frac{n-n_{t}}{2(n_{t}+1)}\right]|n\rangle\langle n|.$$
(16)

By setting $l = l_k = \lfloor (n_t + 1)/2^{k-1} \rfloor$ or $l = l_k = \lceil (n_t + 1)/2^{k-1} \rceil$ for the kth round of evolution and measurement, it is found that $\Pi_e(\tau)$ is almost the same as the non-unitary evolution operator $\mathcal{U}_g(\tau_k)$ in Eq. (5) up to irrelevant local phases

$$\Pi_e(l_k t_{n_t}) \approx \mathcal{U}_q(\tau_k).$$
 (17)

The general parity measurement $\mathcal{M}_{\mathrm{GP}}^{(N)}$ on the resonator can therefore be constructed by N such rounds of evolution and measurement with gradually decreasing intervals. Then $\rho_a(N)$ in Eq. (7) still holds except that P(N) is replaced by

$$P_e(N) \approx \text{Tr} \left[\mathcal{M}_{GP}^{(N)} \rho_a(0) \mathcal{M}_{GP}^{(N)} \right].$$
 (18)

III. LARGE FOCK STATE GENERATION

By leveraging the approximated generalized parity measurement constructed by the circuit in Fig. 1(b), we can efficiently generate a large number state using merely projective measurements on the ancillary TLS, with no additional gate operations on either resonator or ancillary system.

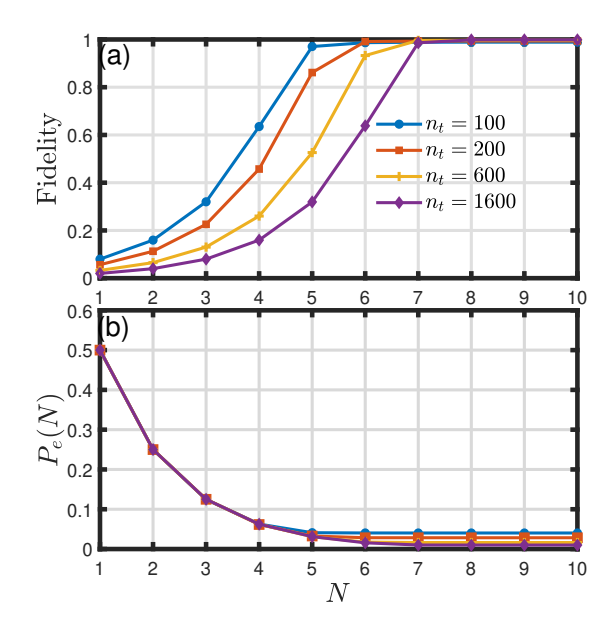


FIG. 2. (a) Fidelity and (b) Success probability as functions of the number N of rounds of free evolution and measurement for various target Fock state $|n_t\rangle$.

In Fig. 2(a), we present the fidelity $F = \langle n_t | \rho_a(N) | n_t \rangle$ of the target Fock states $|n_t\rangle$ with $n_t = 100, 200, 600,$ and 1600 as a function of the measurement number N. The results indicate that the fidelities rapidly converge to nearly unit in less than 10 rounds of measurements across a wide range of n_t . In particular, N=6 and N=8measurements are sufficient to generate $|n_t = 100\rangle$ and $|n_t = 1600\rangle$ with $F \geq 0.99$, respectively. Figure 2(b) demonstrates the relevant success probabilities $P_e(N)$ of finding the gubit at its excited state for all rounds of measurements. The steady-state success probabilities for the generated Fock states with $n_t = 100, 200, 600, and$ 1600 are $P_e \approx 0.04, 0.028, 0.016, 0.009$, respectively. In the absence of decoherence, they are determined by the overlap between the initial coherent state and the target Fock state

$$P_e(N) \to |\langle n_t | \alpha \rangle|^2 = e^{-n_t} \frac{n_t^{n_t}}{n_t!}.$$
 (19)

Using the Stirling formula $n_t! \approx e^{-n_t} n_t^{n_t} \sqrt{2\pi n_t}$, we have $P_e(\infty) \sim 1/\sqrt{2\pi n_t}$ that varies with a small rate for $n_t \gg 1$. Moreover, during the first four rounds, the success probability descends roughly as 2^{-N} , irrespective to n_t . It can be understood by the fact that for a coherent state with $|\alpha|^2 = n_t \gg 1$, the population distribution

is an approximately Gaussian function centered around n_t [30], which is given by

$$|\langle n|\alpha\rangle|^2 \approx \sqrt{\frac{1}{2\pi n_t}} \exp\left[-\frac{(n-n_t)^2}{2n_t}\right].$$
 (20)

After N rounds of measurements, the success probability in Eq. (18) turns out to be

$$P_{e}(N) \approx \operatorname{Tr}\left[\mathcal{M}_{GP}^{(N)}|\alpha\rangle\langle\alpha|\mathcal{M}_{GP}^{(N)}\right]$$

$$= \sqrt{\frac{1}{2\pi n_{t}}} \sum_{j \geq \lfloor -n_{t}/2^{N} \rfloor} \exp\left(-\frac{j^{2}2^{2N}}{2n_{t}}\right), \qquad (21)$$

due to Eq. (8). For $n_t 2^{1-2N} \gg 1$, the summation over j can be approximated by the Gaussian integral

$$\sum_{j \ge \lfloor -n_t/2^N \rfloor} \exp\left(-\frac{j^2}{n_t 2^{1-2N}}\right)$$

$$\approx \int_{-\infty}^{+\infty} \exp\left(-\frac{x^2}{n_t 2^{1-2N}}\right) dx = \sqrt{\pi n_t 2^{1-2N}}.$$
(22)

By inserting Eq. (22) into Eq. (21), it is found that the success probability $P_e(N) \approx 2^{-N}$ in the first several rounds, which is independent of the target state.

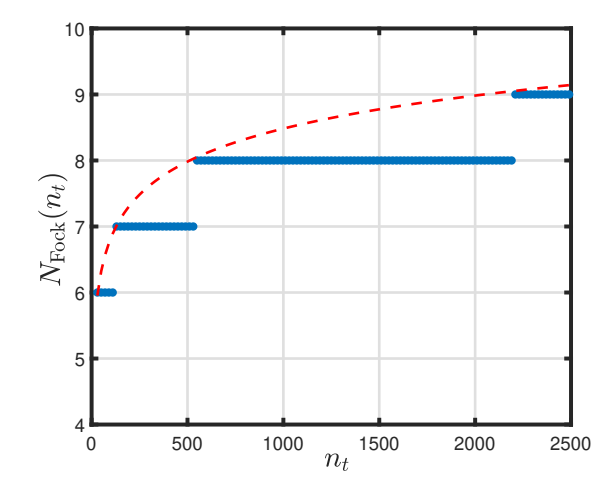


FIG. 3. Number of evolution-measurement rounds for generating a Fock state $|n_t\rangle$ with a fidelity exceeding 98% as a function of the target excitation number n_t . The red dashed line represents the fitting curve $N_{\text{Fock}}(n_t) \approx \log_2(\sqrt{n_t}) + 3.5$.

Figure 3 plots the minimum number of evolution-measurement rounds $N_{\rm Fock}(n_t)$ required to prepare a Fock state $|n_t\rangle$ with a fidelity exceeding 98% against the target excitation number n_t . The blue lines are obtained by the numerical results. The red-dashed line indicates the fitting curve $N_{\rm Fock}(n_t) \approx \log_2(\sqrt{n_t}) + 3.5$ showing that $N_{\rm Fock}(n_t)$ roughly follows a logarithmical function of the square root of n_t , which confirms that our protocol is almost the same as QPE in complexity.

In comparison to the conventional GPM protocols in Fig. 1(a) assisted by the dispersive-coupling between

an ancillary TLS and the target resonator, our protocol in Fig. 1(b) offers at least three advantages in efficiency: (1) The dispersive-coupling approach employs two Hadamard gates per round of evolution and measurement, that is more complex in performance and brings extra amount of gate-infidelity. (2) The total running time of our protocol is $T_{\rm res} \propto \sqrt{n_t}/g$, whereas the time consumption of the dispersive-coupling protocol is $T_{\rm dis} \propto 1/\chi$. It is straightforward to find that the former is faster than the latter as long as $n_t < g^2/\chi^2$. In the current circuit QED platforms with a typical dispersivecoupling strength $\chi \sim 1$ MHz between the superconducting qubit and the microwave cavity and the exchange coupling strength $q \sim 100$ MHz [31–33], our protocol holds the advantage in the cost of running time for generating Fock states within $n_t < 10^4$. (3) In both protocols, the period of each round is set as one half of the last round. Yet one has to tune the detunings Δ for different target states $|n_t\rangle$ in the dispersive-coupling protocol.

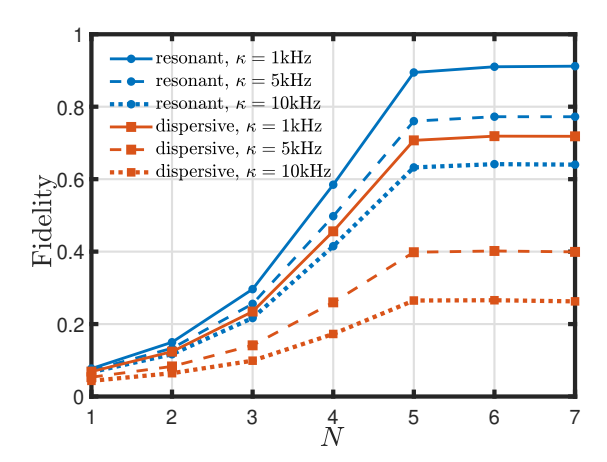


FIG. 4. Comparison of the resonant exchange coupling protocol [Fig. 1(b)] and the dispersive-coupling protocol [Fig. 1(a)] for GPM in generating Fock state $|n_t=100\rangle$ under various cavity decay rates. Here $\gamma=\gamma_\phi=100$ kHz, g=100 MHz, and $\chi=2$ MHz.

In a practical experiment, decoherence and dephasing caused by the surrounding environment would degrade the attainable fidelity of any generated target state. Under a zero-temperature environment, the time evolution of the composite system can be described by the Lindblad master equation

$$\dot{\rho}(t) = -i[H_{\rm JC}, \rho(t)] + \kappa \mathcal{L}[a]\rho(t) + \gamma \mathcal{L}[|g\rangle\langle e|]\rho(t) + \gamma_{\phi}\mathcal{L}[|e\rangle\langle e|]\rho(t),$$
(23)

where γ and κ are the decay rates of the ancillary qubit and target resonator, respectively, γ_{ϕ} is the dephasing rate of the qubit, and $\mathcal{L}[o]$ is the Lindblad superoperator defined as $\mathcal{L}[o]\rho \equiv o\rho o^{\dagger} - 1/2(o^{\dagger}o\rho + \rho o^{\dagger}o)$. In a 3D circuit QED platform, the decay rate of the 3D microwave cavity $\kappa \approx 1-10$ kHz. The qubit relaxation time and dephasing time are about $T_1 \approx T_{\phi} \approx 10-100$ ns. Then $\gamma \approx \gamma_{\phi} \approx 10-100$ kHz [31–33]. Here we assume $\gamma = \gamma_{\phi} = 100$ kHz

for a transmon qubit; and the strength of the resonant and dispersive coupling are set as g=100 MHz, and $\chi=2$ MHz, respectively, in the numerical simulation.

In Fig. 4, we compare the performance of our protocol of approximated GPM in which the target resonator is exchangeably coupled to an ancillary qubit with the dispersive-coupling protocol for three different cavity decav rates $\kappa = 1$, 5, and 10 kHz. As shown in Fig. 4, our resonant-coupling protocol consistently outperforms the dispersive one, exhibiting significantly higher fidelities under various cavity decay rates. After N=7 measurements, the fidelities of the former reach 91%, 77%, and 64% while the fidelities of the latter are about 71%, 40%, and 26% for $\kappa = 1, 5$, and 10 kHz, respectively. The outstanding performance of our protocol mainly stems from the less time consumption of the generation procedure. The output fidelity nearly saturates in both protocols with N = 5 rounds of measurements for generating the Fock state $|n_t = 100\rangle$. Nevertheless, it takes $T_{\rm res} \approx \sum_{k=1}^5 \sqrt{n_t + 1\pi}/(2^{k-1}g) \approx 606$ ns in our protocol, while $T_{\rm dis} = \sum_{k=1}^5 \pi/(2^{k-1}\chi) \approx 3043$ ns in the dispersive-coupling protocol.

IV. PREPARING DICKE STATE VIA GPM

Another advantage of our circuit model in Fig. 1(b) is its versatility in the type of the target states. An effective generalized parity measurement can be constructed to prepare the Dicke state of a large spin-ensemble, which is one of the resource states for quantum metrology [34–38]. Numerous protocols have been proposed for generating the Dicke states in the systems of several qubits [39–43]. However, extending these methods to large scale remains a significant challenge due to the requirement of the individual addressing of the probe qubits or the inner coupling among them, which is costly in a large spin-ensemble, e.g., the diamond nitrogen-vacancy (NV) centers [44]. Our protocol needs merely to locally address and readout the ancillary system, e.g., the central spin in the spin-star model.

A. Effective GPM in spin-star model

Consider a spin-star model consisting of a central spin-1/2 coupled to a spin ensemble containing M identical spin-1/2's via a Heisenberg XY interaction of identical coupling strength [45–48]. The full Hamiltonian reads

$$H = \frac{\omega_c}{2}\sigma_c^z + \frac{\omega_b}{2}\sum_{i=1}^M \sigma_j^z + g\sum_{i=1}^M (\sigma_c^x \sigma_j^x + \sigma_c^y \sigma_j^y), \quad (24)$$

where σ^k 's, k = x, y, z, are the Pauli operators along various directions and g is the spin-spin coupling strength. ω_c and ω_b are the energy splitting of the center spin and

the surrounding spins, respectively. By rewriting the interaction Hamiltonian in terms of the transition operators $\sigma^+ = |e\rangle\langle g|$ and $\sigma^- = |g\rangle\langle e|$ and transforming the full Hamiltonian to the rotating frame with respect to $H_0 = \omega_b/2(\sigma_c^z + \sum_{j=i}^M \sigma_j^z)$, we have

$$H' = \frac{\Delta}{2}\sigma_c^z + 2g\sum_{j=1}^{M} (\sigma_c^+ \sigma_j^- + \sigma_c^- \sigma_j^+)$$

$$= \frac{\Delta}{2}\sigma_c^z + 2g(\sigma_c^+ J_- + \sigma_c^- J_+),$$
(25)

where $\Delta = \omega_c - \omega_b$ is the detuning between the center spin and the spins in the spin ensemble. $J_{\pm} = \sum_{j=1}^{M} \sigma_{j}^{\pm}$ are the collective angular momentum operators. We assume that the state of the spin ensemble is restricted to the permutation symmetric subspace, i.e., the subspace with the total spin J = M/2. Any state $|J, m_t\rangle$ with $-M/2 < m_t < M/2$ in that subspace could be regarded as a general Dicke state. Such model has been considered for generating Dicke state via repeated exchange of excitation between the central spin and the spin ensemble; and each round consists of a flipping on center spin and a half Rabi oscillation of the composite system [38]. Staring from a polarized state $|J, \pm J\rangle$, it is extremely hard for generating the "center" Dick state of a large spin-ensemble $|J = M/2 \gg 1, 0\rangle$.

The collective angular momentum operator J_{\pm} in this subspace can be rewritten as

$$J_{\pm} = \sum_{m=-J}^{J} \sqrt{J(J+1) - m(m\pm 1)} |J, m\pm 1\rangle \langle J, m|.$$

The center spin is supposed to be initially prepared as one of its energy eigenstate $|i\rangle$, i=e,g, and the initial state of the spin ensemble is $\rho_b(0)$. Then the separable initial state of the composite system is

$$\rho(0) = |i\rangle\langle i| \otimes \rho_b(0). \tag{27}$$

Similar to the generation of Fock states, after a period of free evolution $U(\tau) = \exp(-iH'\tau)$, we perform a projective measurement $M_i = |i\rangle\langle i|$ on the center spin. The state of the spin ensemble becomes

$$\rho_b(1) = \frac{V_i(\tau)\rho_b(0)V_i^{\dagger}(\tau)}{P_i(1)},\tag{28}$$

where $P_i(1) = \text{Tr}[V_i(\tau)\rho_b(0)V_i^{\dagger}(\tau)]$ is the success probability of measuring the center spin in state $|i\rangle$, and $\rho_b(N)$ is the density matrix of the spin ensemble after N rounds of measurements. The effective non-unitary evolution operator $V_i(\tau) = \langle i|U(\tau)|i\rangle$ reads

$$V_i(\tau) = \sum_{m=-J}^{J} \lambda_m^{(i)}(\tau) |J, m\rangle \langle J, m|, \qquad (29)$$

where the coefficients $\lambda_m^{(i)}(\tau)$ are given by

$$\lambda_m^{(i)}(\tau) = e^{-i\Delta\tau/2} \left[\cos\left(\Lambda_m^{(i)}\tau\right) + i \frac{\Delta}{2\Lambda_m^{(i)}} \sin\left(\Lambda_m^{(i)}\tau\right) \right],\tag{30}$$

with

$$\Lambda_m^{(g)} = \sqrt{\Delta^2/4 + 4g^2[J(J+1) - m(m-1)]}, \quad (31)$$

$$\Lambda_m^{(e)} = \sqrt{\Delta^2/4 + 4g^2[J(J+1) - m(m+1)]}.$$
 (32)

To hold the population on the target Dicke state $|J, m_t\rangle$, the relevant coefficients have to satisfy $|\lambda_{m_t}^{(i)}(\tau)| = 1$, which renders the evolution period of each round

$$\tau = \xi t_{m_t}^{(i)}, \quad t_{m_t}^{(i)} \equiv \frac{\pi}{\Lambda_{m_t}^{(i)}}$$
 (33)

with $\xi \in \mathbb{N}$. Under the resonant condition $\Delta = 0$, the non-unitary evolution operator for each round of evolution and measurement turns out to be

$$V_{e}(\xi t_{m_{t}}^{(e)}) = \sum_{m=-J}^{J} \cos \left[\xi \pi \sqrt{\frac{J(J+1) - m(m+1)}{J(J+1) - m_{t}(m_{t}+1)}} \right] |J, m\rangle\langle J, m|,$$
(34)

$$V_{g}(\xi t_{m_{t}}^{(g)}) = \sum_{m=-J}^{J} \cos \left[\xi \pi \sqrt{\frac{J(J+1) - m(m-1)}{J(J+1) - m_{t}(m_{t}-1)}} \right] |J, m\rangle\langle J, m|.$$
(35)

Suppose the spin ensemble is initially prepared in the product state $\rho_b(0) = |\psi_b(0)\rangle\langle\psi_b(0)|$, where

$$|\psi_b(0)\rangle = \left[\cos\left(\frac{\phi}{2}\right)|g\rangle + \sin\left(\frac{\phi}{2}\right)|e\rangle\right]^{\otimes M}$$
$$= \sum_{m=-J}^{J} p_M(m)|J,m\rangle, \tag{36}$$

$$p_M(m) = \sqrt{\binom{M}{m+M/2}} \cos^{\frac{M}{2}-m} \left(\frac{\phi}{2}\right) \sin^{\frac{M}{2}+m} \left(\frac{\phi}{2}\right).$$
(37)

The overlap between the initial state and target Dicke state is maximized when $\phi = \arccos(-2m_t/M)$ [49]. In this situation, the populations on the Dicke state components $|J,m\rangle$ with $|m-m_t|\gg \sqrt{M}/2$ are negligible, since the standard deviation of $|p_M(m)|^2$ is $\sqrt{M}/2$ [27]. Thus we can only consider the Dicke state components near the target Dicke state $|J,m_t\rangle$.

For simplicity, we now focus on the generation of the center Dicke state $|J,0\rangle$. The other Dicke state with $m_t/M \ll 1$ can be treated in a similar way. In this case, the non-unitary evolution operators in Eqs. (34) and (35)

can be approximated as

$$V_{i}(\xi t_{0}^{(i)}) = \sum_{m=-J}^{J} \cos \left[\xi \pi \sqrt{1 - \frac{m(m \pm 1)}{J(J+1)}} \right] |J, m\rangle\langle J, m|$$

$$\approx \sum_{m=-J}^{J} \cos \left[\xi \pi - \xi \pi \frac{m(m \pm 1)}{2J(J+1)} \right] |J, m\rangle\langle J, m|$$

$$= \sum_{m=-J}^{J} (-1)^{\xi} \cos \left[\xi \pi \frac{m(m \pm 1)}{2J(J+1)} \right] |J, m\rangle\langle J, m|,$$
(28)

where the upper (lower) sign corresponds to i = e (i = g). By setting $\xi = \xi_k = \lfloor J(J+1)/2^k \rfloor$ or $\lceil J(J+1)/2^k \rceil$ for the kth round of evolution and measurement, the spin ensemble is projected into the subspace spanned by the set of Dicke states $|J,m\rangle$ with $|m(m\pm 1)/2^{N+1}| \in \mathbb{N}$ after N rounds, which is equivalent to preform an effective operator for generalized parity measurement on the spinensemble

$$\rho_b(N) = \frac{\mathcal{P}_i^{(N)} \rho_b(0) \mathcal{P}_i^{(N)}}{P(N)}.$$
 (39)

The effective GPM operator reads,

$$\mathcal{P}_{i}^{(N)} \equiv \sum_{j} \left(|J, 2^{N+1}j\rangle \langle J, 2^{N+1}j| + |J, 2^{N+1}j \mp 1\rangle \langle J, 2^{N+1}j \mp 1| \right).$$

$$(40)$$

Similar to the Fock state generation, the number of measurement rounds for generating a Dicke state nearby the center Dicke state $|J,0\rangle$ roughly scales as $N_{\rm Dicke}(M) \sim \log_2(\sqrt{M})$, since the standard deviation of $|p_M(m)|^2$ is $\sqrt{M}/2$.

B. Dicke state generation

It is straightforward to find from Eq. (40) that the target Dicke state $|J,0\rangle$ cannot be distinguished from $|J,1\rangle$ ($|J,-1\rangle$) by only using the non-unitary evolution operator $V_g(\tau)$ [$V_e(\tau)$]. Thus we can take a hybrid strategy. In the first round, we can prepare the center spin in the excited state $|e\rangle$ and perform the projective measurement $M_e = |e\rangle\langle e|$ on the center spin after a period of $\tau = \xi_1 t_0^{(e)}$ to filter out the population on $|J,1\rangle$. And then we can use a pulse to flip the center spin from $|e\rangle$ to $|g\rangle$ and begin to perform rounds of the evolution and measurement with the duration $\tau = \xi_{k-1} t_0^{(g)}$ and the projective measurement operator $M_g = |g\rangle\langle g|$ in the subsequent kth rounds with $k \geq 2$. Therefore, only an extra single gate is required in our protocol, which is substantially simpler than the standard QPE algorithm [27, 50].

In Fig. 5(a) and 5(b), we present the fidelity $F = \langle J, 0 | \rho_b(N) | J, 0 \rangle$ and the success probability P(N) for generating the Dicke state $|J = M/2, 0\rangle$ with various spin

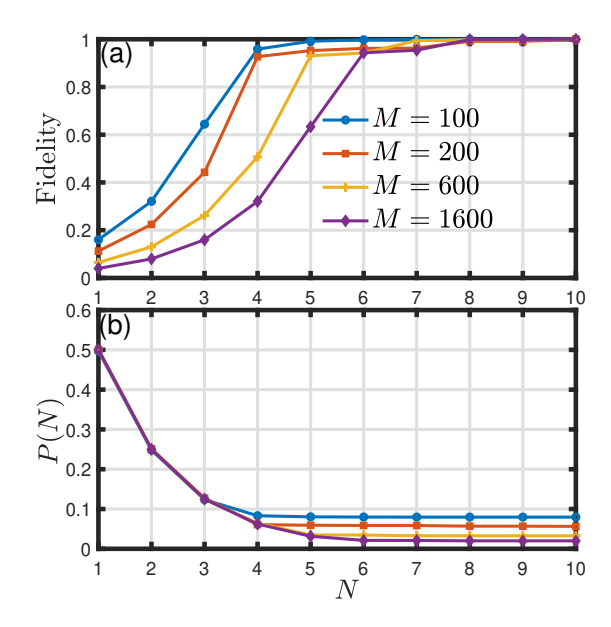


FIG. 5. Dependence of (a) fidelity of center Dicke state $|J,0\rangle$ and (b) success probability on the number rounds N for various spin number M in the spin ensemble.

numbers M, respectively. For a wide range of M=100 to M=1600, the center Dicke state $|J,0\rangle$ can be generated with F>0.99 within 8 rounds of evolution and measurement. Similar to the case of Fock state generation, the asymptotic value of success probabilities are determined by the overlap between the target center Dicke state and the initial product state. Using the Stirling formula, the asymptotic value is found to be

$$P(N) \to |p_M(0)|^2 = {M \choose M/2} 2^{-M} \approx \sqrt{\frac{2}{\pi M}}.$$
 (41)

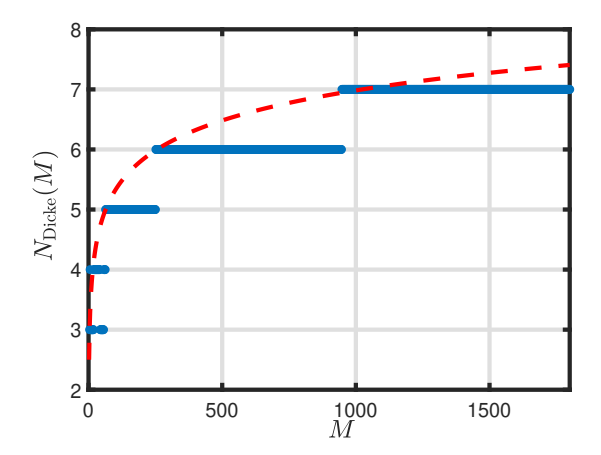


FIG. 6. Number of evolution-measurement rounds for generating center Dicke state with a fidelity exceeding 90% as a function of the size of spin ensemble M. The red dashed line represents the fitting curve $N_{\text{Dicke}}(M) = \log_2(\sqrt{M}) + 2$.

Moreover, due to the similar reason as to the Fock state

generation, the success probability also exhibits an M-independent behavior in the first a few rounds. For $M \gg 1$, the population distribution in the subspace $|p_M(m)|^2$ is found to be approximately a Gaussian function:

$$|p_M(m)|^2 \approx \sqrt{\frac{2}{\pi M}} \exp\left(-\frac{2m^2}{M}\right).$$
 (42)

Owing to the fact that

$$\operatorname{Tr}\left[\mathcal{P}_{i}^{(N)}|\psi_{b}(0)\rangle\langle\psi_{b}(0)|\mathcal{P}_{i}^{(N)}\right]$$

$$=\sqrt{\frac{2}{\pi M}}\sum_{j}\left[\exp\left(-\frac{j^{2}}{M2^{-3-N}}\right)+\exp\left(-\frac{(j\pm1)^{2}}{M2^{-3-N}}\right)\right]$$

$$\approx2\sqrt{\frac{2}{\pi M}}\int_{-\infty}^{+\infty}dx\exp\left(-\frac{x^{2}}{M2^{-3-N}}\right)=2^{-N}$$
(43)

under the condition $M \gg 2^{3+N}$, the success probability is about 2^{-N} .

Figure (6) presents the number $N_{\text{Dicke}}(M)$ of rounds required by our protocol for generating Dicke state $|J,0\rangle$ with J=M/2 as a function of spin number M. The reddashed line is a fit curve with $N_{\text{Dicke}} = \log_2(\sqrt{M}) + 2$, which confirms an approximate logarithmic scaling supported by GPM or QPE.

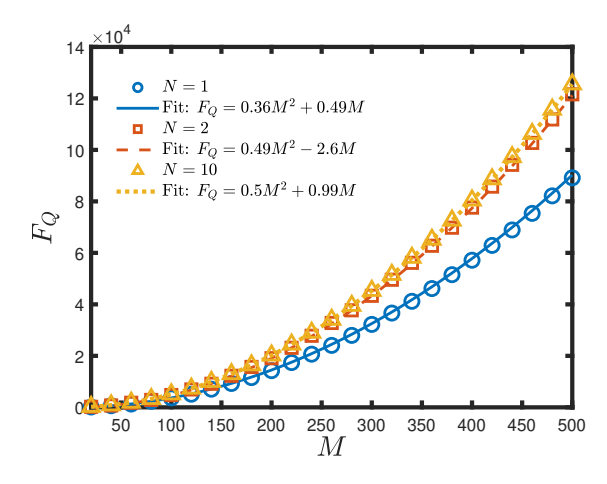


FIG. 7. Quantum Fisher information for estimating the phase θ along the x direction as a function of the spin-probe size M after N rounds of evolution and measurements.

To apply the state generated by our protocol to quantum metrology, it is not necessary to attain an extremely high-fidelity Dicke state by a lot of repeated measurements. Here we calculate the quantum Fisher information (QFI) [51] for estimating the phase θ along the x direction encoded by $R_x(\theta) = \exp(-i\theta J_x)$ to the probe spin ensemble. In our protocol for generating Dicke state, the state of the spin ensemble remains in a pure state. Consequently, QFI of the output state for estimating θ is given

by $F_Q = 4\langle \psi_b(N)|J_x^2|\psi_b(N)\rangle - 4|\langle \psi_b(N)|J_x|\psi_b(N)\rangle|^2$, where $|\psi_b(N)\rangle$ is the practical state of the spin ensemble after N rounds of evolution and measurement obtained by Eq. (39). For an ideal center Dicke state $|J=M/2,0\rangle$ of a spin ensemble containing M spins, QFI is found to be $F_Q(M) = M^2/2 + M$ [34].

In Fig. (7), we plot QFI as a function of the ensemble size M after N=1 (blue circles), N=2 (red squares), and N=6 (yellow triangles) rounds of evolution and measurement. In each case, the data are well described by a quadratic fit of the form $F_Q(M) \approx aM^2 + bM$. It is interesting to find that QFI exhibits a significantly faster convergence rate than the fidelity in Fig. (5). For N=2, the factor a for the square term has already approached the ideal value 1/2 for the Heisenberg limit in metrology precision.

V. CONCLUSION

We have presented a measurement-based protocol for the efficient preparation of nonclassical states with large number of excitations in bosonic and spin-ensemble systems via the resonant interaction between the ancillary qubit and the target system and repeated projective measurement on the ancillary qubit. By repeatedly performing evolution-measurement rounds with carefully tailored duration of the joint-evolution in each round, one can construct an effective generalized-parity measurement that projects the target system onto large Fock states or large Dicke states. Our analysis proves that the required number of rounds grows only logarithmically with the square root of the target excitation number, which is the same as the schemes assisted by quantum phase estimation algorithm or Ramsey interference. While our protocol is much simpler than them with much less number of operations. Numerical simulations adopting realistic cavity and qubit decoherence rates confirm that high-fidelity Fock states can be generated in 6 measurement cycles for the excitation number over 100. Moreover, our protocol provides a simple method to generate an approximate Dicke state, which can achieve a Heisenberg scaling behavior in quantum Fisher information with only 2 rounds of measurement. This work demonstrates that the generalized parity measurement could become a powerful and practical tool for quantum state engineering.

ACKNOWLEDGMENT

We acknowledge grant support from the Science and Technology Program of Zhejiang Province (No. 2025C01028).

- [1] B. Misra and E. C. G. Sudarshan, The zeno's paradox in quantum theory, J. Math. Phys. 18, 756 (1977).
- [2] D. Home and M. Whitaker, A conceptual analysis of quantum zeno; paradox, measurement, and experiment, Ann. Phys. (NY) 258, 237 (1997).
- [3] W. M. Itano, D. J. Heinzen, J. J. Bollinger, and D. J. Wineland, *Quantum zeno effect*, Phys. Rev. A 41, 2295 (1990).
- [4] J.-M. Zhang, J. Jing, L.-G. Wang, and S.-Y. Zhu, Criterion for quantum zeno and anti-zeno effects, Phys. Rev. A 98, 012135 (2018).
- [5] H. Nakazato, T. Takazawa, and K. Yuasa, Purification through zeno-like measurements, Phys. Rev. Lett. 90, 060401 (2003).
- [6] H. Nakazato, M. Unoki, and K. Yuasa, Preparation and entanglement purification of qubits through zeno-like measurements, Phys. Rev. A 70, 012303 (2004).
- [7] L.-A. Wu, D. A. Lidar, and S. Schneider, Longrange entanglement generation via frequent measurements, Phys. Rev. A 70, 032322 (2004).
- [8] G. Vacanti and A. Beige, Cooling atoms into entangled states, New J. Phys. 11, 083008 (2009).
- [9] N. Qiu, S.-c. Wang, L. C. Kwek, and X.-B. Wang, Preparation and entanglement purification through twostep measurements, Phys. Rev. A 86, 012313 (2012).
- [10] J. Busch, S. De, S. S. Ivanov, B. T. Torosov, T. P. Spiller, and A. Beige, Cooling atom-cavity systems into entangled states, Phys. Rev. A 84, 022316 (2011).
- [11] Y. Li, L.-A. Wu, Y.-D. Wang, and L.-P. Yang, Nondeterministic ultrafast ground-state cooling of a mechanical resonator, Phys. Rev. B 84, 094502 (2011).
- [12] R. Puebla, O. Abah, and M. Paternostro, Measurement-based cooling of a nonlinear mechanical resonator, Phys. Rev. B 101, 245410 (2020).
- [13] P. V. Pyshkin, D.-W. Luo, J. Q. You, and L.-A. Wu, Ground-state cooling of quantum systems via a one-shot measurement, Phys. Rev. A 93, 032120 (2016).
- [14] J.-s. Yan and J. Jing, External-level assisted cooling by measurement, Phys. Rev. A 104, 063105 (2021).
- [15] T. K. Konar, S. Ghosh, and A. Sen(De), Refrigeration via purification through repeated measurements, Phys. Rev. A 106, 022616 (2022).
- [16] L.-A. Wu, Nuclear spin polarization and manipulation by repeated measurements, J. Phys. A: Math. Theor. 44, 325302 (2011).
- [17] Z.-y. Jin, J.-s. Yan, and J. Jing, Measurement-induced nuclear spin polarization, Phys. Rev. A 106, 062605 (2022).
- [18] J.-s. Yan and J. Jing, Charging by quantum measurement, Phys. Rev. Appl. 19, 064069 (2023).
- [19] D. S. Abrams and S. Lloyd, Quantum algorithm providing exponential speed increase for finding eigenvalues and eigenvectors, Phys. Rev. Lett. 83, 5162 (1999).
- [20] A. Kitaev, Fault-tolerant quantum computation by anyons, Ann. Phys. (NY) 303, 2 (2003).
- [21] M. A. Nielsen and I. L. Chuang, Quantum Computation and Quantum Information: 10th Anniversary Edition (Cambridge University Press, 2010).
- [22] N. F. Ramsey, A molecular beam resonance method with separated oscillating fields, Phys. Rev. 78, 695 (1950).

- [23] A. Y. Kitaev, Quantum measurements and the abelian stabilizer problem, arXiv:quant-ph/9511026.
- [24] T. E. O'Brien, B. Tarasinski, and B. M. Terhal, Quantum phase estimation of multiple eigenvalues for small-scale (noisy) experiments, New J.Phys. 21, 023022 (2019).
- [25] B. M. Terhal and D. Weigand, Encoding a qubit into a cavity mode in circuit qed using phase estimation, Phys. Rev. A 93, 012315 (2016).
- [26] K. Duivenvoorden, B. M. Terhal, and D. Weigand, Single-mode displacement sensor, Phys. Rev. A 95, 012305 (2017).
- [27] Y. Wang and B. M. Terhal, Preparing dicke states in a spin ensemble using phase estimation, Phys. Rev. A 104, 032407 (2021).
- [28] X. Deng, S. Li, Z.-J. Chen, Z. Ni, Y. Cai, J. Mai, L. Zhang, P. Zheng, H. Yu, C.-L. Zou, S. Liu, F. Yan, Y. Xu, and D. Yu, Quantum-enhanced metrology with large fock states, Nat. Phys. 20 (2024).
- [29] W.-L. Ma, S.-S. Li, and R.-B. Liu, Sequential generalized measurements: Asymptotics, typicality, and emergent projective measurements, Phys. Rev. A 107, 012217 (2023).
- [30] S. Barnett and D. Pegg, On the hermitian optical phase operator, J. Mod. Opt. 36, 7 (1989).
- [31] M. Hofheinz, E. M. Weig, M. Ansmann, R. C. Bialczak, E. Lucero, M. Neeley, A. D. O'Connell, H. Wang, J. M. Martinis, and A. N. Cleland, Generation of fock states in a superconducting quantum circuit, Nature (London) 454, 310 (2008).
- [32] W. Wang, L. Hu, Y. Xu, K. Liu, Y. Ma, S.-B. Zheng, R. Vijay, Y. P. Song, L.-M. Duan, and L. Sun, Converting quasiclassical states into arbitrary fock state superpositions in a superconducting circuit, Phys. Rev. Lett. 118, 223604 (2017).
- [33] T. Brecht, Y. Chu, C. Axline, W. Pfaff, J. Z. Blumoff, K. Chou, L. Krayzman, L. Frunzio, and R. J. Schoelkopf, Micromachined integrated quantum circuit containing a superconducting qubit, Phys. Rev. Appl. 7, 044018 (2017).
- [34] G. Tóth, Multipartite entanglement and high-precision metrology, Phys. Rev. A 85, 022322 (2012).
- [35] Z. Zhang and L. M. Duan, Quantum metrology with dicke squeezed states, New J. Phys. 16, 103037 (2014).
- [36] I. Apellaniz, B. Lücke, J. Peise, C. Klempt, and G. Tóth, Detecting metrologically useful entanglement in the vicinity of dicke states, New J. Phys. 17, 083027 (2015).
- [37] L. Pezzè, A. Smerzi, M. K. Oberthaler, R. Schmied, and P. Treutlein, Quantum metrology with nonclassical states of atomic ensembles, Rev. Mod. Phys. 90, 035005 (2018).
- [38] H. Hakoshima and Y. Matsuzaki, Efficient detection of inhomogeneous magnetic fields from a single spin with dicke states, Phys. Rev. A 102, 042610 (2020).
- [39] L.-M. Duan and H. J. Kimble, Efficient engineering of multiatom entanglement through single-photon detections, Phys. Rev. Lett. 90, 253601 (2003).
- [40] R. Ionicioiu, A. E. Popescu, W. J. Munro, and T. P. Spiller, Generalized parity measurements, Phys. Rev. A 78, 052326 (2008).
- [41] L. Lamata, C. E. López, B. P. Lanyon, T. Bastin, J. C. Retamal, and E. Solano, Deterministic generation

- of arbitrary symmetric states and entanglement classes, Phys. Rev. A 87, 032325 (2013).
- [42] C. Wu, C. Guo, Y. Wang, G. Wang, X.-L. Feng, and J.-L. Chen, Generation of dicke states in the ultrastrong-coupling regime of circuit qed systems, Phys. Rev. A 95, 013845 (2017).
- [43] V. M. Stojanović and J. K. Nauth, Dicke-state preparation through global transverse control of ising-coupled qubits, Phys. Rev. A 108, 012608 (2023).
- [44] F. Dolde, V. Bergholm, Y. Wang, I. Jakobi, B. Naydenov, S. Pezzagna, J. Meijer, F. Jelezko, P. Neumann, T. Schulte-Herbrüggen, et al., Highfidelity spin entanglement using optimal control, Nat. Commun. 5, 3371 (2014).
- [45] J. Jing and Z. Lü, Dynamics of two qubits in a spin bath with anisotropic xy coupling, Phys. Rev. B **75**, 174425 (2007).

- [46] A. Hutton and S. Bose, Mediated entanglement and correlations in a star network of interacting spins, Phys. Rev. A 69, 042312 (2004).
- [47] H.-P. Breuer, D. Burgarth, and F. Petruccione, Non-markovian dynamics in a spin star system: Exact solution and approximation techniques, Phys. Rev. B 70, 045323 (2004).
- [48] C. Radhakrishnan, Z. Lü, J. Jing, and T. Byrnes, Dynamics of quantum coherence in a spin-star system: Bipartite initial state and coherence distribution, Phys. Rev. A 100, 042333 (2019).
- [49] O. Nagib, M. Saffman, and K. Mølmer, Efficient preparation of entangled states in cavity qed with grover's algorithm, Phys. Rev. Lett. 135, 050601 (2025).
- [50] L. Piroli, G. Styliaris, and J. I. Cirac, Approximating many-body quantum states with quantum circuits and measurements, Phys. Rev. Lett. 133, 230401 (2024).
- [51] S. L. Braunstein and C. M. Caves, Statistical distance and the geometry of quantum states, Phys. Rev. Lett. 72, 3439 (1994).